Clara Lauscher

Alexander Licau

Gerhard Schaldach

Markus Thommes*

Characterization of Sprays Generated by the Expansion of Emulsions with Liquid Carbon Dioxide

Expanding emulsions with liquid CO_2 facilitates the creation of aerosols with an average droplet diameter in the low micrometer size range, which is challenging with conventional atomizers. The droplet formation process of the expansion of high-pressure emulsions was investigated using a plain-orifice atomizer and different swirl nozzles. The local droplet size and droplet velocities were measured and used to estimate the local Weber number and thus infer the droplet size reduction. Measurements of the local mass concentration in the aerosol showed that, for the swirl nozzle, the highest concentration was found outside of the central axis, indicating radial momentum generated by the swirl nozzle. Furthermore, it was shown that the type of expansion nozzle used has an influence on the resulting median droplet size in the aerosol. For a water mass load of 0.01, the median droplet diameter was reduced from 8 to 3 µm by increasing the swirl number from 0.01 to 0.1.

1   Introduction

Small droplets are used in a variety of fields due to their high specific surface. The greater surface area in comparison to bulk benefits the mass and energy transfer and, thus, chemical reactions can be accelerated or cooling and drying processes can be improved. Furthermore, atomization processes can be used in painting processes, agricultural methods, humidification processes, fuel technology, drug application, and spray drying [1, 2].

Especially in spray drying, droplets in the small micrometer size range are often desired. However, with conventional atomizers, it is rather challenging to produce droplets in this size range due to limitations in workability [3, 4]. Therefore, in a previous study [5], an approach for producing droplets in this size range was described. An emulsion of water in liquid CO_2 was produced by jetting the water into the liquid CO_2 through an orifice. Afterwards, the high-pressure emulsion was expanded through a second orifice with a low length-to-diameter ratio, enabling a rapid decrease of the pressure, resulting in the evaporation of the liquid CO_2 and a breakup of the water droplets. A schematic illustration of the generation of an aerosol of the water droplets in gaseous CO_2 is shown in Fig. 1.

The expansion of emulsions with water and liquid CO_2 allows the generation of median droplet diameters between 3 and 10 µm for water mass loads between 0.01 and 0.08. An increasing droplet diameter with increasing water mass load was observed, which was traced back to the decreasing specific energy input. The energy input is mainly provided by the expanding CO_2, and it was quantified with the enthalpy difference between the liquid and the gaseous CO_2.

In the investigation, it was shown that the smallest droplets were measured in the center area of the spray cone. However, the measured median droplet diameters in the center were integrated values over the entire radius of the spray cone due to the applied laser diffraction technique. Knowledge of the local droplet sizes in the spray cone is nevertheless essential for a better understanding of droplet formation during the expansion process. With the usage of phase-Doppler anemometry, it is possible to determine the local droplet size; moreover, a local velocity can be assigned to each droplet, which gives additional insights into the expansion process of the CO_2 and the possible resulting acceleration of the water droplets.

The expansion of the high-pressure emulsion through a variety of orifices was investigated, along with no variation of the expansion nozzle type. The single-fluid nozzle providing the smallest median droplet diameter is usually the pressure swirl nozzle [4]. There, grooves in the swirl generator force the liquid into a swirl motion, leading to a rotation around the central

M.Sc. Clara Lauscher, B. Sc. Alexander Licau, Dipl.-Chem. Gerhard Schaldach, Prof. Dr. rer. nat. Markus Thommes (professors.fsv.bci@tu-dortmund.de)
TU Dortmund University, Laboratory of Solids Process Engineering, Emil-Figge-Straße 68, 44227 Dortmund, Germany.
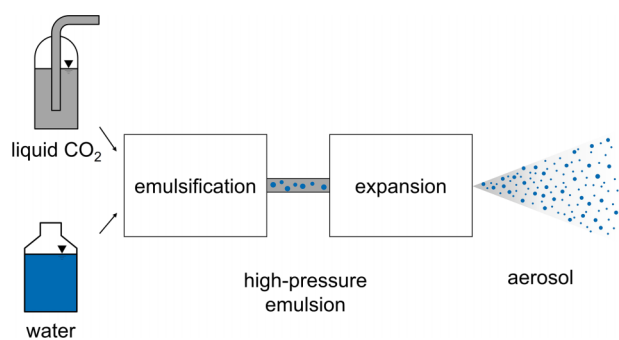
Figure 1. Schematic illustration of the investigated approach for the production of small droplets.

axis of the nozzle. Due to the centrifugal force, the liquid is pressed to the wall and an air cone is formed. The liquid at the wall forms a thin film, which exits the nozzle in the form of a thin lamella. Depending on the fluid velocity and the resulting disintegration regime, the lamella then disintegrates into small droplets close to the opening of the nozzle or further downstream.

The swirl generator can be characterized by the swirl number Δ, which indicates the ratio of the tangential momentum to the axial momentum (Eq. (1)). In the equation, r_{KE} is the mean inlet radius, D is the diameter of the nozzle, A_E is the total area of all inlet cross sections, and β is the angle of inclination of the inlet channels [6].

$$\Delta = \frac{\pi r_{KE} D}{4 A_E} \cos(\beta) \qquad (1)$$

Thus, the usage of a swirl nozzle instead of an orifice could reduce the droplet size in the aerosol. However, whether a lamella of the emulsion is formed or not still needs to be investigated. This would require a delayed expansion and evaporation process of the liquid CO_2.

The aim of the presented study is an experimental investigation of the droplet formation process when expanding emulsions with liquid CO_2. Therefore, the experimental setup to generate and characterize the aerosols, as well as the results, will be presented, and the latter will be discussed. The local droplet sizes and velocities as well as the local mass concentration are of particular interest. In the first sections, the focus will be on the usage of the plain orifice as an expansion nozzle, before the comparison to the swirl nozzle is made and discussed.

2 Materials and Methods

The experimental setup is shown in Fig. 2. The ultra-pure water and the liquid CO_2 (technical CO_2; Messer Industriegase, Bad Soden, Germany) were pumped with a high-performance liquid chromatography (HPLC) pump (80 P; Knauer, Berlin, Germany) and a gas dosing station (DSD/500/3.2/So; Maximator, Nordhausen, Germany), respectively. Both liquids were injected into the cylindrical mixing chamber with an inner diameter of 10 mm and

a length of 30 mm. The water was inserted through an orifice with a diameter of 100 μm, with volume flow rates between 0.072 and 1.5 kg h^{-1}. The liquid CO_2 was pumped through an orifice with a diameter of 500 μm, with a mass flow rate of 7.45 kg h^{-1}, which equals water mass loads between 0.01 and 0.21. The two emulsification nozzles were positioned at a 90° angle and a distance of 1 mm to each other. Afterwards, the produced high-pressure emulsion was expanded through either a plain orifice with a diameter of 200 μm or a pressure swirl nozzle, also with an opening diameter of 200 μm (model 121; Düsen-Schlick GmbH, Untersiemau, Germany) and different swirl chambers. Based on the geometrical properties of the swirl nozzles, swirl numbers of 0.01, 0.05, and 0.1 were determined according to Eq. (1).

The measurements of the droplet size in the aerosol by laser diffraction (Spraytec; Malvern Instruments, Malvern, UK) were conducted at a distance of 350 mm to the expansion nozzle. Each measurement was performed for a time interval of at least 30 s, resulting in an average of 30 droplet size distributions. A distortion of the droplet size measurements by the evaporating CO_2 was prevented [7].

A phase-Doppler anemometer (FiberFlow; Dantec Dynamics, Skovlunde, Dänemark) with transmitting and receiving optics 57X80 was used to evaluate the droplet size measurements and the droplet velocity measurement with a high local resolution. Measurement points in axial distances to the expansion nozzle between 20 and 350 mm were selected. The radial measurement positions were selected in accordance with a spray angle of about 30°. A rotational symmetry of the spray cone was assumed, and for each position, 9000 droplets were measured.

3 Results and Discussion

3.1 Droplet Size and Velocity Measurements

3.1.1 Influence of the Axial Position in the Spray Cone

The droplet sizes and velocities were measured in different axial positions in the radial center of the spray cone. The median droplet sizes for the three water mass loads are shown in Fig. 3. In accordance with the previous publication [5], the
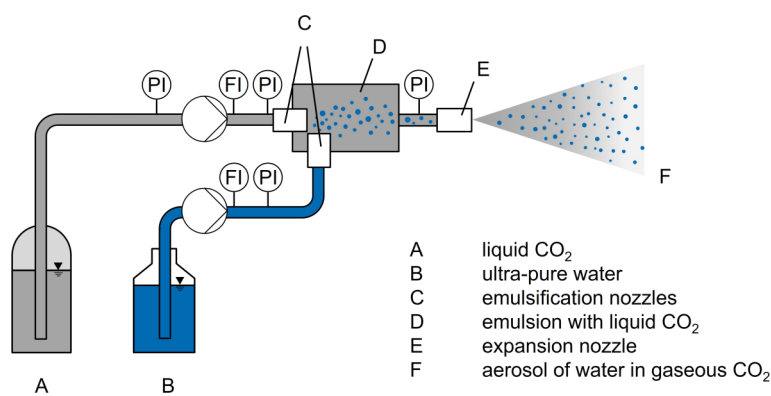

A	liquid CO_2
B	ultra-pure water
C	emulsification nozzles
D	emulsion with liquid CO_2
E	expansion nozzle
F	aerosol of water in gaseous CO_2

Figure 2. Experimental setup.

highest median droplet diameters were measured for the highest water mass load, due to the decreasing specific energy with increasing water mass load. For all water mass loads, the largest droplets with median droplet diameters between 21 and 36 µm were measured close to the expansion nozzle at a distance of 20 mm. In general, smaller droplets were measured with increasing distance to the expansion nozzle. At a distance of 350 mm from the expansion nozzle, median droplet diameters between 7 and 11 µm were determined.
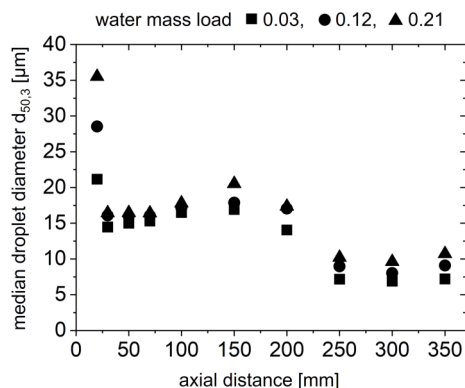

Figure 3. Median droplet diameter as a function of the axial distance to the expansion nozzle in the center of the spray cone for water mass loads of 0.03, 0.12, and 0.21.

Representative droplet velocities are shown in Fig. 4 for the water mass load of 0.12 and different droplet sizes of 0.5, 9.5, 19.5, and 30.5 µm. Close to the expansion nozzle at an axial position of 20 mm, droplet velocities between 27 and 51 m s^{-1} were measured. Except for the droplet size of 0.5 µm, the droplet velocity in this region increased with increasing droplet size. A plausibility check was carried out by calculating the velocity of the liquid emulsion through the expansion nozzle under the assumption of a constant density. For a density of the emulsion of 869 kg m^{-3}, a mean outlet velocity of 85 m s^{-1} can be calculated, which is higher than the measured maximum value at an axial distance of 20 mm downstream.
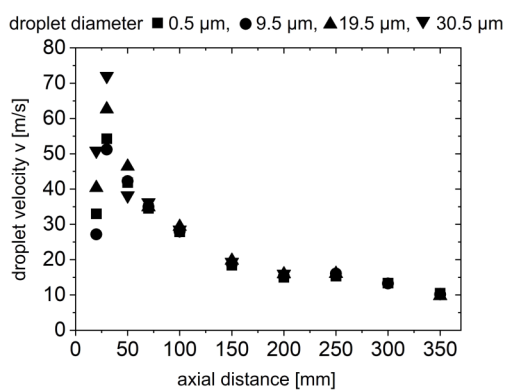

Figure 4. Droplet velocity as a function of the axial distance to the expansion nozzle in the center of the spray cone for droplet diameters of 0.5, 9.5, 19.5, and 30.5 µm and a water mass load of 0.12.

The velocity decrease might be due to the entrainment of the surrounding air and the corresponding impulse transmission. Due to the higher inertia force of the larger droplets, their velocity decreases more slowly, leading to the higher remaining velocity at the axial distance of 20 mm. The assumption of a liquid emulsion exiting the nozzle and an expansion of the CO_2 outside of the nozzle leading to an acceleration of the droplets could explain the slight increase in droplet velocity at an axial position between 20 and 30 mm. In addition, an acceleration of the droplets due to evaporation of the CO_2 could explain the higher droplet velocity of the 0.5-µm droplets in comparison to the 9.5-µm droplets at an axial distance of 30 mm.

With further increasing axial distance to the expansion nozzle, the droplet velocity decreased until the velocity of all shown droplet sizes reached a value of about 10 m s^{-1} at an axial distance of 350 mm to the expansion nozzle. The deceleration of the droplets can again be explained with increasing entrainment of the surrounding air and the corresponding impulse transmission leading to all droplets moving with the same velocity.

In general, droplets with a diameter of about 1 µm possess a low inertia and take on the velocity of the surrounding fluid after a short time [8]. Quantitatively, this can be expressed by the relaxation time, which corresponds to the time after which a droplet reaches 63 % of its final velocity. The relation is shown in Eq. (2). Here, ρ is the density of the droplet, d is the diameter, and μ is the viscosity of the surrounding fluid, CO_2 [9].

$$\tau_d = \frac{\rho_d d^2}{18\mu} \qquad (2)$$

For droplets with a diameter of 0.5 µm, a relaxation time of about 1 µs with a corresponding travelled distance of about 60 µm can now be determined, which justifies the assumption that droplets of this size follow the gas stream and can thus be assumed to have the same velocity as the gas.

On that basis, the relative velocity between the larger droplet classes and the gas velocity was determined and subsequently used to estimate the droplet Weber numbers. The droplet Weber number relates the inertial force to the surface force and can be understood as the degree of droplet deformation (Eq. (3)). In addition to the relative velocity $v_{relative}$, the surface tension σ is also taken into account. Above a critical Weber number, the deforming forces exceed the form-retaining ones, leading to droplet breakup.

$$We = \frac{\rho v_{relative}^2 d}{\sigma} \qquad (3)$$

According to the literature, the critical Weber number for a free-falling droplet is around 13 [10, 11].

In Fig. 5, the resulting droplet Weber number is shown for a droplet size of 30.5 µm as a function of the axial distance from the expansion nozzle. Close to the expansion nozzle, Weber numbers of up to 133 were reached, which could explain the droplet size reduction between axial distances of 20 and 30 mm in Fig. 3. However, the droplet size reduction between axial dis-
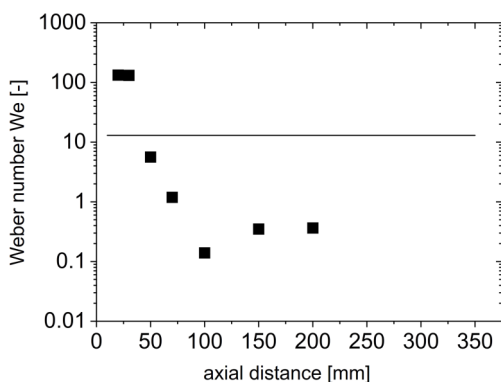
Figure 5. Local Weber number of droplets with a diameter of 30.5 μm as a function of the axial distance to the expansion nozzle in the center of the spray cone for a water mass load of 0.12; line: critical Weber number for a free-falling drop.

tances of 150 and 250 mm cannot be explained with the local droplet Weber number. For this second droplet size reduction, drying effects can be assumed, but then a steady reduction of the droplet diameter with increasing time, and thus with increasing axial distance, would be expected. The constant droplet diameter from an axial distance of 250 mm thus contradicts the assumption of drying effects.

3.1.2 Influence of the Radial Position in the Spray Cone

The influence of the radial position in the spray cone on the median droplet diameter is shown in Fig. 6a. For the shorter axial distance of 70 mm, the highest median droplet diameters were measured at the edge of the spray cone, due to the lower relative velocity. Thus, a similar trend as in the previous paper could be observed. For an axial distance of 350 mm, however, the median droplet diameter appears to be rather similar for all radial positions. Thus, the mixing seems to be completed in the radial direction at this distance.

A well-equalized droplet velocity in the spray cone at an axial distance of 350 mm was observed (Fig. 6b). In addition to the

droplets of 9.5 μm shown here, the other droplet sizes also exhibit velocities of about 10 m s^{-1}, regardless of their radial position. The droplets with a diameter of 0.5 μm show the same velocity; so, the gas velocity can be assumed for all droplets in the spray cone at this axial distance.

3.2 Mass Flow Density Distribution

The characterization of the atomization process through an orifice was completed with the consideration of local mass concentration in the aerosol. Therefore, the local number density was convolved with the droplet size distribution. The results are shown in Fig. 7 as a function of the radial distance to the center of the spray, for different axial distances to the expansion nozzle. For a better visualization, the measurement results were normalized to the maximum value. At an axial distance of 100 mm to the expansion nozzle, the highest mass concentration was determined in the radial center of the spray cone. This trend, as well as the calculated spray angle of about 28°, corresponds to the measurement presented in the previous publication [5]. However, at an axial distance
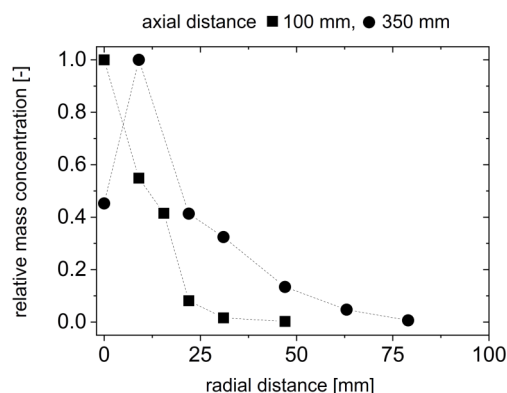

Figure 7. Normalized mass concentration as a function of the axial position in the spray cone at the axial positions of 100 and 350 mm for a water mass load of 0.12.
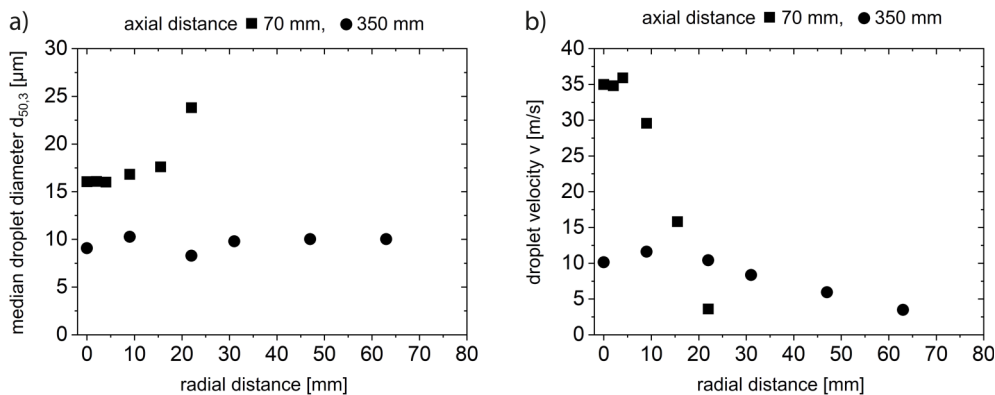

Figure 6. (a) Median droplet size as a function of the radial distance to the center for axial distances of 70 and 350 mm for a water mass load of 0.12; (b) droplet velocity (d = 9.5 μm) as a function of the radial distance to the center for axial distances of 70 and 350 mm.

of 350 mm, the maximum mass concentration was measured slightly outside of the axial center, which could be caused by turbulences with the surrounding air. This local minimum does not necessarily contradict the results in the previous paper, since in the previous paper, the scattering signal was based on the measurement of a cylindrical volume with a diameter of about 1 cm through the spray cone, and thus small minima and maxima were not visible. Based on the measurement at an axial distance of about 350 mm, a spray angle of about 20° was calculated.

3.3 Comparison with the Swirl Nozzle

To investigate the influence of the swirl number, the median droplet sizes were measured by laser diffraction at an axial distance of 350 mm to the expansion nozzle. The results are shown in Fig. 8 as a function of the water mass load and for the different swirl numbers. As already seen for the nozzle with the plain orifice, the median droplet diameter increased with increasing water mass load. Furthermore, a droplet size reduction can be observed with increasing swirl number. While a median droplet diameter of 9 μm was measured with the swirl number of 0.01, the median droplet diameter was reduced to 6 and 4 μm by the stronger swirl inserts of 0.05 and 0.1, respectively, for a water mass load of 0.05.
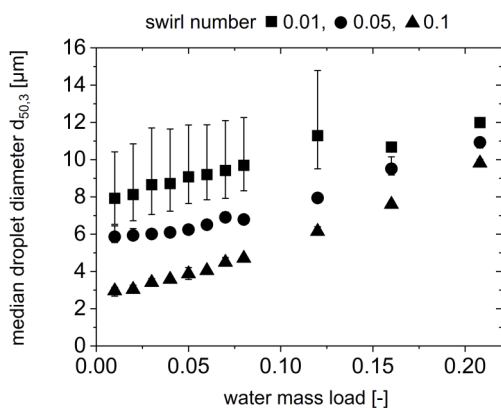
Figure 8. Median droplet size at a distance of 350 mm from the expansion nozzle as a function of the water mass load for different swirl numbers (measured by laser diffraction; min., av., max.; $n = 3$).

For the swirl numbers of 0.01 and 0.1, further measurements were conducted to investigate a potential difference from the plain orifice. The median droplet diameter as a function of the radial position for an axial distance of 350 mm is shown in Fig. 9. In accordance with Fig. 8, the median droplet diameter for the higher swirl number is smaller. However, an influence of the radial distance on the median droplet diameter was not observed for the two different swirl numbers in this position of the spray cone.

For comparison, the median droplet diameters measured by laser diffraction were also added (horizontal dotted line). The results of laser diffraction and phase-Doppler anemometry
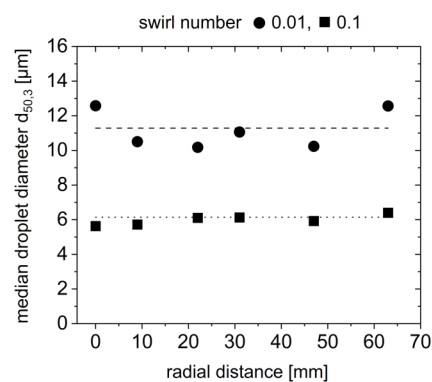
Figure 9. Median droplet size at a distance of 350 mm from the expansion nozzle as a function of the radial position in the spray cone for swirl numbers of 0.01 and 0.1 and a water mass load of 0.12; dashed and dotted line: measurements by laser diffraction.

show acceptable agreement, and the measurement methods can thus be verified.

As no influence of the swirl number on the median droplet diameter in radial direction was observed, the influence of the swirl chamber on the spray pattern was investigated. In particular, it was investigated whether the emulsion of water in liquid CO_2 was leaving the nozzle with a tangential velocity component and to what extent a hollow cone was formed. For this purpose, the relative mass density in the spray cone was also determined for the swirl number of 0.1. The results are shown in Fig. 10. At the short axial distance of 100 mm, the maximum value of the relative mass was not measured in the center; so, a hollow cone can be assumed. Furthermore, it can also be assumed that the emulsion exits the nozzle in a liquid state. This is also supported by the fact that the nozzle does not cool down during atomization.

For a further investigation on the effect of the swirl, the atomization efficiency was calculated for the three swirl nozzles and the orifice, according to the equation presented in [5]. As the droplet size has a strong impact on the atomization efficiency, the efficiencies were calculated for a fixed droplet size of about 9.5 μm. The results are shown in Fig. 10b. The atomization efficiency of the swirl nozzles is in the same order of magnitude as the one of the orifices. A detailed comparison was not carried out as the nozzles had the same diameter but slightly different geometries. The atomization efficiency of the swirl nozzles increased with increasing swirl number. This could be explained by a thinner lamella, which accordingly also decays to smaller droplets, also indicating that the CO_2 exits the nozzle in the liquid state.

4 Conclusion

An investigation into the droplet formation process during the expansion of emulsions with liquid CO_2 was carried out. The high-pressure emulsion was produced in a mixing chamber via two orifices arranged at an angle of 90° to each other, through which water and liquid CO_2 were pumped. Subsequently, the emulsion was expanded through a plain orifice with a diameter
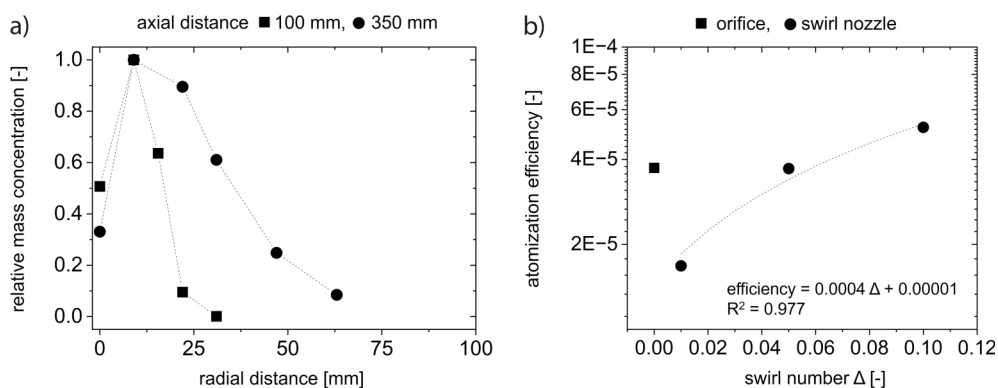
Figure 10. (a) Normalized mass concentration as a function of the radial position in the spray cone for the swirl nozzle with a swirl number of 0.1 and a water mass load of 0.12 for two axial positions; (b) dependency of the atomization efficiencies of droplets of $9.5\,\mu m$ in diameter on the swirl number.

of $200\,\mu m$ or, alternatively, through various swirl nozzles also with an orifice diameter of $200\,\mu m$ and swirl numbers of 0.01, 0.05, and 0.1. Using a phase-Doppler anemometer, the local droplet diameters, droplet velocities, and mass concentrations were measured. The highest droplet diameters of $21–35\,\mu m$ for water mass loads between 0.03 and 0.21 were measured close to the expansion nozzle. At an axial distance of $350\,mm$ from the nozzle tip, smaller droplets with an average droplet diameter of $7–11\,\mu m$ were measured. The droplet size reduction could be explained in part by the calculated droplet Weber numbers. In the radial direction, the smallest median droplet diameter was measured in the center of the spray cone. In the axial direction, mixing occurred to such an extent that this trend was no longer recognizable at the axial distance of $350\,mm$.

The highest droplet velocities were also measured close to the expansion nozzle. The droplets were accelerated, presumably by the expanding CO_2. With increasing distance from the expansion nozzle, the droplets slowed down due to mixing with the surrounding air in the axial radial directions. At an axial distance of $350\,mm$, the deceleration of the droplets and the mixing had progressed to such an extent that all the droplets had the same velocity of $10\,m\,s^{-1}$.

The highest water mass concentration for both the orifice plate and the swirl inserts was not measured in the spray axis but slightly outside, with this effect being more pronounced for the swirl inserts. With higher swirl numbers, smaller droplets could be produced, due to a presumably smaller lamella of the liquid emulsion. The atomization efficiency is on the same order of magnitude as the one calculated for the plain-orifice nozzle. A linear relationship was found for the dependency of the dimensionless atomization efficiency on the dimensionless swirl number. With an increasing tangential velocity component at the exit of the swirl nozzle, the atomization efficiency increases.

Acknowledgment

Symbols used

A_E	[m^2]	total area of all inlet cross-sections
d	[m]	droplet diameter
D	[m]	nozzle diameter
r_{KE}	[m]	mean inlet radius
v	[m s^{-1}]	velocity
We	[–]	Weber number

Greek symbols

β	[°]	angle of inclination of the grooves
Δ	[–]	swirl number
μ	[kg m^{-1}s^{-1}]	viscosity
ρ	[kg m^{-3}]	density
σ	[kg s^{-2}]	surface tension

References

[1] G. Wozniak, *Zerstäubungstechnik*, Springer, Berlin, Heidelberg **2003**.

[2] N. Ashgriz, *Handbook of Atomization and Sprays*, Springer US, Boston **2011**.

[3] P. Walzel, in *Ullmann's Encyclopedia of Industrial Chemistry*, Wiley-VCH Verlag, Weinheim **2000**.

[4] P. Walzel, *Design of Spraying Devices I; Short Course on Atomization and Sprays*, Darmstadt **2017**.

[5] C. Lauscher, G. Schaldach, M. Thommes, *Atomization Sprays* **2022**, *32 (4)*, 77–93. DOI: https://doi.org/10.1615/AtomizSpr.2022039582

[6] E. Musemic, Experimentelle Untersuchungen zum Tropfenbildungsprozess an Hohlkegeldüsen, *Ph.D. Thesis*, TU Dortmund, Dortmund **2013**.

[7] A. Mescher, P. Walzel, *Chem. Ing. Tech.* **2010**, *82 (5)*, 717–722. DOI: https://doi.org/10.1002/cite.200900166

[8] G. Rudinger, A. Chang, *Phys. Fluids* **1964**, *7 (11)*, 1747. DOI: https://doi.org/10.1063/1.2746772

[9] A. G. Laptev, M. M. Basharov, T. M. Farakhov, A. R. Iskhakov, *Adv. Chem. Eng. Sci.* **2014**, *4 (2)*, 143–148. DOI: https://doi.org/10.4236/aces.2014.42017

[10] J. O. Hinze, *AIChE J.* **1955**, *1 (3)*, 289–295.

[11] A. H. Lefebvre, V. G. McDonell, *Atomization and Sprays*, CRC Press, Boca Raton **2017**.